Journal of Power Sources 196 (2011) 504–507

Contents lists available at ScienceDirect

Journal of Power Sources

journal homepage: www.elsevier.com/locate/jpowsour

Short communication

Hydrogen storage properties of lithium silicon alloy synthesized by mechanical alloying

Koichi Doi[a], Satoshi Hino[b], Hiroki Miyaoka[b], Takayuki Ichikawa[a,b,*], Yoshitsugu Kojima[a,b]

[a] Graduate School of Advanced Sciences of Matter, Hiroshima University, 1-3-1 Kagamiyama, Higashi-Hiroshima 739-8530, Japan
[b] Institute for Advanced Materials Research, Hiroshima University, 1-3-1 Kagamiyama, Higashi-Hiroshima 739-8530, Japan

ARTICLE INFO

Article history:
Received 22 February 2010
Received in revised form 16 May 2010
Accepted 19 May 2010
Available online 26 June 2010

Keywords:
Hydrogen storage
Mechanical alloying
Thermodynamics
Light elements
Lithium ion battery
Negative electrode

ABSTRACT

A lithium silicon alloy was synthesized by mechanical alloying method. Hydrogen storage properties of this Li–Si–H system were studied. During hydrogenation of the lithium silicon alloy, lithium atom was extracted from the alloy and lithium hydride was generated. Equilibrium hydrogen pressures for desorption and absorption reactions were measured in a temperature range from 400 to 500 °C to investigate the thermodynamic characteristics of the system, which can reversibly store 5.4 mass% hydrogen with smaller reaction enthalpy than simple metal Li. Li absorbing alloys, which have been widely studied as a negative electrode material for Li ion rechargeable batteries, can be used as hydrogen storage materials with high hydrogen capacity.

1. Introduction

Thermodynamic properties of lithium–silicon alloys and their hydrogen (H_2) absorption and desorption properties were investigated. Utilization of H_2 as an energy carrier in a transport sector contributes to reduction of CO_2 emission. H_2 storage technique is one of the key factors for practical use of fuel cell vehicles [1]. H_2 can be stored in materials with high volumetric H_2 density, compared to compressed gas or liquid H_2. The requirements for H_2 storage materials also include appropriate thermodynamics, fast kinetics, high gravimetric densities and long cycle lifetime. Thermodynamics and kinetics have a significant influence on the temperature for H_2 release. The targets of performance, set by US Department of Energy's Office of Energy Efficiency and Renewable Energy, are gravimetric H_2 density of >9 mass% and operating temperature range of −40 to 85 °C [2]. Recently, H_2 storage materials composed of light elements, such as NH_3BH_3 [3], AlH_3 [4] and NH_3 [5,6], have been investigated due to the advantage of high gravimetric H_2 density. These materials have high H_2 capacity and relatively low temperature for H_2 release. However, NH_3BH_3 and AlH_3 show poor reversibility and NH_3 shows toxicity and a pungent odor.

Our group has reported that lithium intercalated graphite LiC_6 can absorb and desorb H_2 through the following reaction [7]:

$$xLiH + 6C \leftrightarrow Li_xC_6 + (x/2)H_2. \quad (1)$$

LiH is stable and desorbs H_2 over 600 °C. However, H_2 can be desorbed via the reaction (1) in the temperature range from 200 to 500 °C. Thus, thermodynamics of H_2 desorption can be controlled by using LiC_6, that is thermodynamically more stable than elemental Li [8], in dehydrogenated state. In the reaction (1), it is noted that absorption/desorption of Li atom into/from (C_6) unit causes desorption/absorption of H_2 gas. Such Li absorbing materials have been studied in details as anode materials for Li-ion batteries (LIB), *e.g.*, LiC_6 [9], $Li_{4.4}Si$ [10], $Li_{4.4}Sn$ [11]. Potentials (V *vs.* Li/Li^+) for lithiation of these materials have been reported to be a positive value, and therefore, Li absorbing alloys should be more stable than Li. A decrease of temperature for H_2 release can be expected by use of the Li absorbing alloys as dehydrogenated materials.

This study has focused on Li–Si alloy. Si as negative electrode material for LIBs has extremely higher theoretical capacity (4200 mAh g^{-1}) than graphite (372 mAh g^{-1}) due to high lithium packing density [12]. It corresponds to Li/Si ratio of 4.4, where the higher ratio causes the higher H_2 capacity when the alloy is used for H_2 storage. During electrochemical insertion of Li into Si, stable intermediate phases, *i.e.*, $Li_{12}Si_7$ ($Li_{1.71}Si$), Li_7Si_3 ($Li_{2.33}Si$), $Li_{13}Si_4$ ($Li_{3.25}Si$), and $Li_{22}Si_5$ ($Li_{4.4}Si$), has been reported [13].

Li–Si alloy, which should be thermodynamically more stable than LiC_6, was used to demonstrate a reversible H_2 storage system

* Corresponding author at: Institute for Advanced Materials Research, Hiroshima University, 1-3-1 Kagamiyama, Higashi-Hiroshima 739-8530, Japan.
Tel.: +81 82 424 5744; fax: +81 82 424 5744.
E-mail address: tichi@hiroshima-u.ac.jp (T. Ichikawa).

0378-7753/$ – see front matter © 2010 Elsevier B.V. All rights reserved.
doi:10.1016/j.jpowsour.2010.05.070

with high capacity through the following reaction in this work:

$$xLiH + Si \leftrightarrow Li_xSi + (x/2)H_2. \quad (2)$$

In previous studies, the pressure of H_2 liberated from a mixture of LiH and Si has been measured and the thermodynamic characteristics of Li_2Si has been estimated [14]. Vajo et al. have reported on the destabilization of LiH with Si [15], where mixture of LiH and Si as a starting material was prepared using mechanical milling. In this work, a mixture of Li and Si was mechanically alloyed and then this alloy was used as a starting material to investigate H_2 storage properties.

2. Experimental

Li–Si alloy was synthesized by the mechanical alloying apparatus (P7, Fritsch) from Li (99.9%, Sigma–Aldrich Co.) and Si (99.999%, Kojundo Chemical Lab. Co., Ltd.) with a 4:1 molar ratio under 0.1 MPa Ar atmosphere for 2 h. Handling of all the chemicals took place in a glove-box filled with purified Ar to avoid being exposed to air and moisture. A powder X-ray diffraction measurement (XRD, RINT-2500V, Rigaku) was performed to identify phases in the samples. The X-ray source was Cu Kα (λ = 1.54 Å). To avoid oxidization during measurement, the sample was covered with a polyimide sheet (Kapton®, Du Pont-Toray Co., Ltd.). H_2 pressure-composition isotherms (PCIs) were measured using a Sieverts type apparatus (Suzuki Shokan Co., Ltd.).

3. Results and discussion

Powder XRD profile of synthesized Li–Si alloy is shown in Fig. 1(a). No diffraction peak corresponding to pristine Li and Si is found. In addition, the profile does not match with any XRD pattern in the ICDD-PDF database. Therefore, we suppose an unknown Li–Si phase (cubic, a = 18.58 Å) appears. The Li–Si alloy was heat-treated at 300 °C under 3 MPa H_2 atmosphere for 8 h to absorb H_2. Fig. 1(b) shows XRD profile of the product after the heat treatment, suggesting that hydrogenation of the Li–Si alloy occurs and LiH and Si are generated. Then, this product was heat-treated at 400 °C under vacuum for 8 h to desorb H_2. As shown in Fig. 1(c), XRD profile of this product indicates that $Li_{2.33}Si$ is generated as the dehydrogenated state. A small amount of LiH remains unreacted, suggesting that heat treatment at higher temperature is needed for a complete dehydrogenation. Fig. 1(d) shows XRD profile of the same product after heat treatment at 500 °C, which is higher than 400 °C, under vacuum for 8 h as dehydrogenated state, suggesting the product is a mixed phase of $Li_{3.25}Si$ and $Li_{4.4}Si$ after dehydrogenation.

Pressure-composition isotherms were measured to determine thermodynamic properties of H_2 absorption and desorption for the Li–Si alloy. After mechanically alloying the samples of Li and Si with 4:1 molar ratio, the sample was hydrogenated and dehydrogenated at 300 and 400 °C, respectively. The product was provided for PCI measurements at 400, 450 and 500 °C. The samples in vessels were evacuated during heating to the measurement temperatures. Since the system showed fast kinetics in both absorption and desorption measurements, a sufficient waiting time for the equilibrium was around 5 min. PCI profile of H_2 absorption to Li–Si alloy at 400 °C as shown in Fig. 2(a) exhibits two plateaus at 0.002 and 0.017 MPa. Considering the XRD results after heating the sample at 400 °C, initial materials for the PCI measurement at 400 °C should be a mixture of $Li_{2.33}Si$ and a small amount of LiH. The widths of the plateau regions are 1.0 and 2.9 mass%, which should correspond to phase transformations from $Li_{2.33}Si + 1.67LiH + 1.165H_2$ (3.9 mass%) to $Li_{1.71}Si + 2.29LiH + 0.855H_2$ (2.9 mass%), and to 4LiH + Si. At 450 °C, two plateaus also appear at 0.007 and 0.054 MPa. The width of the plateau region indicates the same phase transformation as occurred

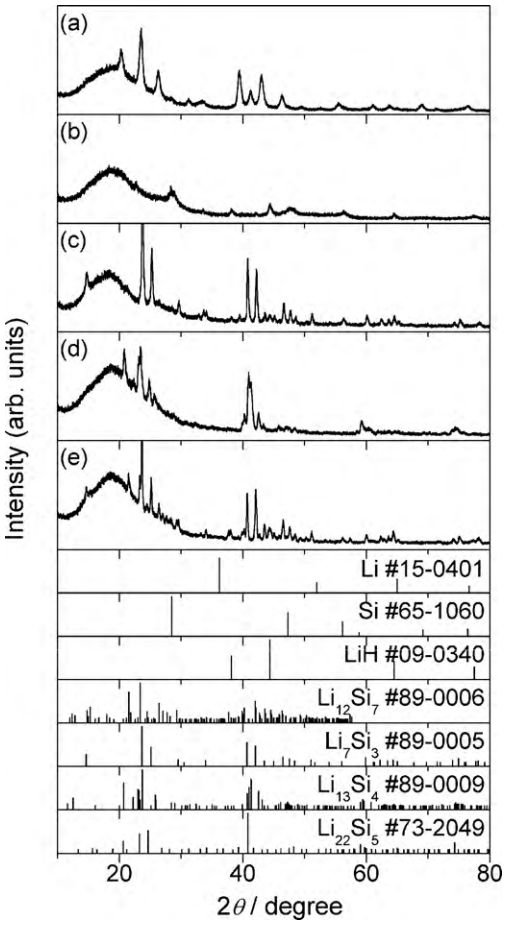

Fig. 1. Powder X-ray diffraction profiles of products (a) after milling of Li and Si with a 4:1 molar ratio for 2 h, (b) after hydrogenation at 300 °C, (c) after dehydrogenation at 400 °C, (d) after dehydrogenation at 500 °C, and (e) after hydrogenation PCI measurement at 500 °C to 2.0 mass% H_2. The peak positions of the typical reflections in the ICDD-PDFs are included for comparison: Li (#15-0401), Si (#65-1060), LiH (#09-0340), $Li_{1.71}Si$ ($Li_{12}Si_7$; #89-0006), $Li_{2.33}Si$ (Li_7Si_3; #89-0005), $Li_{3.25}Si$ ($Li_{13}Si_4$; #89-0009), $Li_{4.4}Si$ ($Li_{22}Si_5$; #73-2049). An upturn of the background at low angle is due to glue used to fix the powder on a sample holder.

for 400 °C. The lower plateau starts at H_2 content of 0.5 mass%, and, additional 0.5 mass% H_2 absorption indicate that starting material could contain a small amount of $Li_{3.25}Si$. In desorption PCI, one plateau corresponding to the phase transformation from LiH + Si to $Li_{1.71}Si$ is observed at 400 and 450 °C in Fig. 2(a) and (b), respectively.

PCI profiles of H_2 absorption at 500 °C shows three plateaus at 0.001, 0.028, 0.162 MPa. The higher two plateaus correspond to the same reactions as those of 400 and 450 °C. The low plateau comes from phase transformation from $Li_{3.25}Si + 0.75LiH + 0.46H_2$ (1.6 mass%) to $Li_{2.33}Si + 1.67LiH$. At 500 °C, $Li_{3.25}Si$ should be included as initial phases, because heat treatment at 500 °C can produce $Li_{3.25}Si$ as shown in Fig. 1(d). Thus, reversible H_2 absorption/desorption reaction of the Li–Si–H system can be described as follows:

$$Li_{3.25}Si + 0.75LiH + 1.625H_2 \leftrightarrow Li_{2.33}Si + 1.67LiH + 1.165H_2 \quad (3)$$

$$Li_{3.25}Si + 0.75LiH + 1.625H_2 \leftrightarrow Li_{1.71}Si + 2.29LiH + 0.855H_2 \quad (4)$$

$$Li_{3.25}Si + 0.75LiH + 1.625H_2 \leftrightarrow 4LiH + Si \quad (5)$$

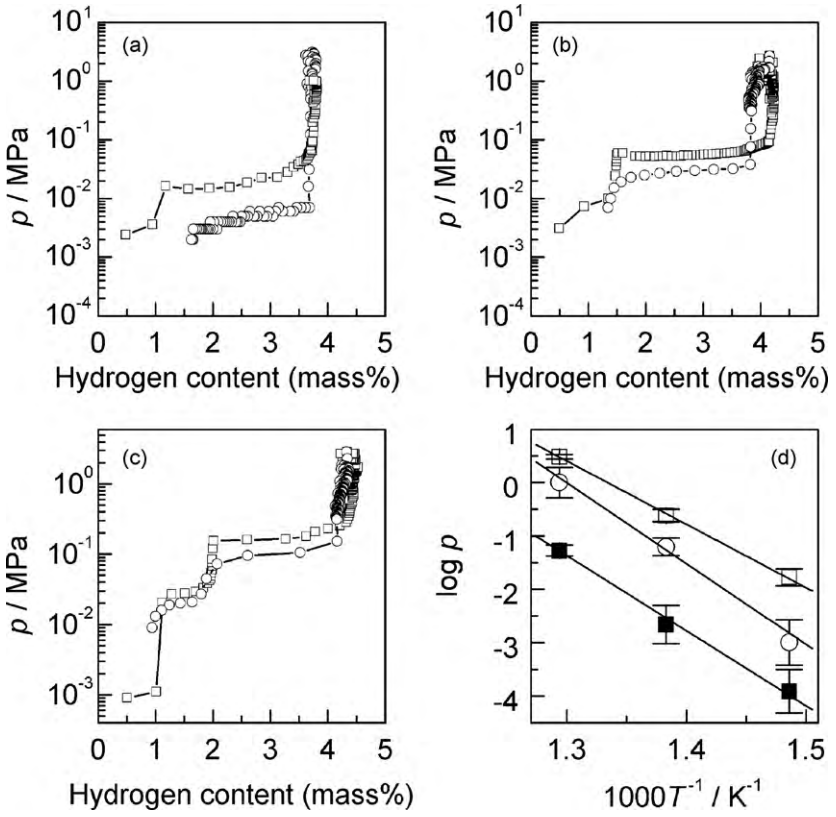

Fig. 2. Pressure-composition isotherms for the Li–Si–H system (circles; desorption, square; absorption) at (a) 400, (b) 450, and (c) 500 °C. (d) Van't Hoff plot of plateau pressures (circles; desorption, open square; absorption: higher plateau, closed square; absorption: lower plateau).

5.4 mass% of H_2 can be stored through the reaction above and, in principle, $Li_{3.25}Si$ can store 6.0 mass% H_2 without excess 0.75LiH. XRD results confirm the LiH and Si as a fully hydrogenated state (Fig. 1(b)), and, $Li_{2.33}Si$ (Fig. 1(c)) and $Li_{3.25}Si$ (Fig. 1(d)) as partially hydrogenated intermediate phases. Fig. 1(e) shows XRD profile of a partially hydrogenated product with 2.0 mass% H_2 absorbed at 500 °C. $Li_{1.71}Si$ is observed as an intermediate phase. Higher plateaus in PCI measured at each temperature show hysteresis which could be caused by heterogeneous solid state reaction or volume change due to phase transformation between Si and $Li_{1.71}Si$.

Fig. 2(d) shows van't Hoff plot ($\ln p$ *vs.* T^{-1}) for the plateau pressures of H_2 absorption and desorption. Gradient and intercept of least-square fit of the plot gives the changes of enthalpy ΔH^o and entropy ΔS^o for the reaction. The results are $\Delta H^o = -99 \pm 6\,kJ\,(mol\,H_2)^{-1}$ and $\Delta S^o = -132 \pm 8\,J\,(mol\,H_2)^{-1}\,K^{-1}$ for the absorption reaction (5), $\Delta H^o = -117 \pm 16\,kJ\,(mol\,H_2)^{-1}$ and $\Delta S^o = -141 \pm 20\,J\,(mol\,H_2)^{-1}\,K^{-1}$ for the absorption reaction (4), $\Delta H^o = 126 \pm 20\,kJ\,(mol\,H_2)^{-1}$ and $\Delta S^o = 164 \pm 30\,J\,(mol\,H_2)\,K^{-1}$ for the desorption reaction (5). These enthalpy values are in good agreement with the reported values [15]. Since the enthalpy change of the decomposition reaction of LiH; $2LiH \rightarrow 2Li + H_2$, is $181\,kJ\,(mol\,H_2)^{-1}$, formation of the Li–Si alloy enables H_2 release by less energy. The ΔS^o value is larger than entropy of gaseous H_2, *i.e.*, $\sim 130\,J\,mol^{-1}\,K^{-1}$. This would be due to large entropy of the Li_xSi alloy compared with LiH and Si, because the configuration number of Li in the alloy could be high. Furthermore, as mentioned above, the hysteresis at higher plateaus in the PCI profiles leads to the difference in the reaction enthalpies corresponding to the absorption and the desorption. Actually, the endothermic process of the desorption reaction could be affected by the heterogeneous process or volume change due to phase transformation, leading to a pseudo equilibrium state of the system. Therefore, in the following discussion, the enthalpies (ΔH^o) and entropies (ΔS^o) corresponding to the absorbing reactions were adopted. Standard enthalpy

Table 1
Thermodynamic functions of reactions and compounds.

Reaction	ΔH^o (kJ (mol H_2)$^{-1}$)		ΔS^o (J (mol H_2)$^{-1}$ K^{-1})	
	This work	Reference	This work	Reference
$Li_{1.71}Si + 2.29LiH + 0.855H_2 \rightarrow 4LiH + Si$	-99 ± 6	-106.5[15]	-132 ± 8	–
$Li_{2.33}Si + 1.67LiH + 1.165H_2 \rightarrow Li_{1.71}Si + 2.29LiH + 0.855H_2$	-117 ± 16	-119.3[15]	-141 ± 20	–

Compound	$\Delta^f H^o$ (kJ mol^{-1})		S^o (J mol^{-1} K^{-1})	
	This work	Reference	This work	Reference
$Li_{1.71}Si$	-71 ± 5	–	54 ± 7	–
$Li_{2.33}Si$	-90 ± 7	–	70 ± 10	–
LiH	–	-90.5[16]	–	20.04[16]
Si	–	0[16]	–	18.8[16]
H_2 (gas)	–	0[16]	–	130.68[16]

of formation ΔH_f^o and standard entropy S^o of the Li–Si alloys can be evaluated from ΔH^o and ΔS^o above and ΔH_f^o and S^o values obtained from the literature [16] as shown in Table 1. The $\Delta^f H^o$ values are derived as follows: $\Delta^f H^o$ ($Li_{1.71}Si$) = -71 ± 5 kJ mol^{-1}, $\Delta^f H^o$ ($Li_{2.33}Si$) = -90 ± 7 kJ mol^{-1}, S^o ($Li_{1.71}Si$) = 54 ± 7 J mol^{-1} K^{-1}, S^o ($Li_{2.33}Si$) = 70 ± 10 J mol^{-1} K^{-1}. Li–Si alloy is indeed more stable than Li or Si, and the stability becomes large with increasing number of Li atom per Si atom in the alloy.

4. Conclusions

H_2 storage properties of Li–Si alloy have been investigated in this work. The Li–Si alloy has been synthesized by mechanical alloying of Li and Si with a 4:1 molar ratio. The XRD profile of the product shows that unknown Li–Si alloy phase is generated. PCI and XRD measurement reveals that reversible H_2 absorption and desorption reactions of the Li–Si alloy are accompanied by the phase transformations of the Li–Si alloy, *i.e.*, $Li_{3.25}Si$ ($Li_{13}Si_4$) ↔ $Li_{2.33}Si$ (Li_7Si_3) ↔ $Li_{1.71}Si$ ($Li_{12}Si_7$) ↔ Si. The Li–Si alloy can store 5.4 mass% H_2 via these reactions, and the reaction enthalpy is reduced by around 60 kJ (mol H_2)$^{-1}$ than that of LiH.

Acknowledgement

This work was partially supported by KAKENHI (21686068) of the Grant-in-Aid for Young Scientists (A) and the project "Advanced Fundamental Research on Hydrogen Storage Materials" of the New Energy and Industrial Technology Development Organization (NEDO). The authors gratefully acknowledge Dr. Masami Tsubota, and Mr. Yasuhiro Matsumura for their help in this work.

References

[1] C.L. Aardahl, S.D. Rassat, Int. J. Hydrogen Energy 34 (2009) 6676–6683.
[2] S. Satyapal, J. Petrovic, C. Read, G. Thomas, G. Ordaz, Catal. Today 120 (2007) 246–256.
[3] M. Chandra, Q. Xu, J. Power Sources 156 (2006) 190–194.
[4] G. Sandrock, J. Reilly, J. Graetz, W.-M. Zhou, J. Johnson, J. Wegrzyn, J. Alloys Compd. 421 (2006) 185–189.
[5] Y. Kojima, K. Tange, S. Hino, S. Isobe, M. Tsubota, K. Nakamura, M. Nakatake, H. Miyaoka, H. Yamamoto, T. Ichikawa, J. Mater. Res. 24 (2009) 2185–2190.
[6] H. Yamamoto, H. Miyaoka, S. Hino, H. Nakanishi, T. Ichikawa, Y. Kojima, Int. J. Hydrogen Energy 34 (2009) 9760–9764.
[7] W. Ishida, H. Miyaoka, T. Ichikawa, Y. Kojima, Carbon 46 (2008) 1628.
[8] Y.F. Reynier, R. Yazami, B. Fultz, J. Electrochem. Soc. 151 (2004) A422–A426.
[9] R. Yazami, K. Zaghib, M. Deschamps, J. Power Sources 52 (1994) 55–59.
[10] S.-J. Lee, J.-K. Lee, S.-H. Chung, H.-Y. Lee, S.-M. Lee, H.-K. Baik, J. Power Sources 97–98 (2001) 191–193.
[11] K. Hirai, T. Ichitsubo, T. Uda, A. Miyazaki, S. Yagi, E. Matsubara, Acta Mater. 56 (2008) 1539–1545.
[12] J. Hassoun, S. Panero, B. Scrosati, Fuel Cells 9 (2009) 277–283.
[13] R.A. Sharma, R.N. Seefurth, J. Electrochem. Soc. 123 (1976) 1763–1768.
[14] Y.M. Dergachev, T.A. Elizarova, N.A. Grechanaya, Zh. Neorg. Khim. 27 (1982) 2451–2453.
[15] J.J. Vajo, F. Mertens, C.C. Ahn, R.C. Bowman, B. Fultz, J. Phys. Chem. B 108 (2004) 13977–13983.
[16] M.W. Chase Jr. (Ed.), NIST-JANAF Themochemical Tables, fourth ed., J. Phys. Chem. Ref. Data, Monograph 9, 1998.